Is Scanning Electron Microscopy/Energy Dispersive X-ray Spectrometry (SEM/EDS) Quantitative? Effects of Specimen Shape

Dale E. Newbury and Nicholas W. M. Ritchie
National Institute of Standards and Technology, Gaithersburg, MD 20899-8370

ABSTRACT

The extraordinary throughput of the silicon drift detector energy dispersive x-ray spectrometer (SDD-EDS) enables collection of EDS spectra with much higher integrated counts within practical time periods, e.g., 100 s or less, compared to past experience with the Si(Li)-EDS. Such high count SDD spectra, containing one million to ten million counts, yield characteristic peak intensities with relative standard deviation below 0.25%, a precision similar to that achieved with wavelength dispersive spectrometry (WDS), the "gold standard" of microprobe analysis, but at lower dose because of the greater solid angle of the SDD-EDS. Such high count SDD-EDS spectra also enable more accurate quantification, nearly indistinguishable from WDS for major and minor constituents when the WDS unknown-to-standard intensity ratio ("k-value") protocol is followed. A critical requirement to satisfy this measurement protocol is that the specimen must be a highly polished bulk target. The geometric character of specimens examined in the scanning electron microscope (SEM) often deviates greatly from the ideal flat bulk target but EDS spectra can still be readily obtained and analyzed. The influence of geometric factors such as local inclination and surface topography on the accuracy of quantitative EDS analysis is examined. Normalized concentration values are subject to very large errors, as high as a factor of 10, as a result of deviation of the specimen geometry from the ideal flat bulk target.

Keywords: Elemental analysis, energy dispersive x-ray spectrometry (EDS), scanning electron microscopy (SEM), silicon drift detector energy dispersive x-ray spectrometer (SDD-EDS), quantitative analysis, x-ray microanalysis

1. INTRODUCTION

Elemental microanalysis by electron-excited x-ray spectrometry has been a key method for characterization in electron beam instruments such as the scanning electron microscope (SEM) for 60 years.[1] Initially, x-ray spectral intensities were measured with the wavelength dispersive spectrometer (WDS), a diffraction-based focusing device that required precisely locating the electron-excited x-ray source on the specimen at the point of maximum transmission to achieve a reproducible measurement of the x-ray intensity, which is a fundamental requirement for establishing a quantitative protocol. Deviation of the x-ray source from the ideal maximum efficiency position by only a few micrometers to tens of micrometers along any axis resulted in severe attenuation of the x-ray signal. Such a stringent criterion for WDS measurements could only be satisfied by a specimen that was polished flat and precisely positioned with the aid of an optical microscope with a shallow depth of focus.[2] When the semiconductor energy dispersive spectrometer (EDS) based upon lithium-drifted silicon [Si(Li)-EDS)] was introduced to the SEM, two of its particular advantages over WDS were its non-focusing, direct line-of-sight acceptance of x-rays and its large solid angle of collection.[3] These properties of EDS made it possible to easily obtain x-ray spectra from the irregularly shaped specimens commonly encountered in scanning electron microscopy that were not readily measureable by WDS.

Early in the development of Si(Li)-EDS it was established that accurate quantitative analysis could be achieved by following the protocol for quantitative analysis previously developed for the WDS, the so-called "k-value method".[4] In the WDS k-value method, the characteristic x-ray peak of each element in the unknown is measured against that same element/peak in a standard of known composition under identical conditions of beam energy, known electron dose, and spectrometer characteristics to form an intensity ratio or k-value. These k-values are converted to concentration ratios (relative to the standards) by applying a set of "matrix correction factors" that account for differences between standards and unknown in the physics of the electron interactions, x-ray generation and x-ray propagation through the specimen to the detector. By following this k-value/matrix correction protocol, EDS analysis was demonstrated to be capable of

Scanning Microscopies 2011: Advanced Microscopy Technologies for Defense, Homeland Security, Forensic, Life, Environmental, and Industrial Sciences, edited by Michael T. Postek, Dale E. Newbury, S. Frank Platek, David C. Joy, Tim K. Maugel, Proc. of SPIE Vol. 8036, 803602 · © 2011 SPIE · CCC code: 0277-786X/11/$18 · doi: 10.1117/12.881040

quantitative results at a similar level of accuracy to that achieved with WDS for major* and minor* constituents provided there were no significant EDS spectral overlaps.[4]

The main limitation of Si(Li)-EDS to routinely achieving high performance quantitative analysis has been its limited x-ray throughput. The detector time constant determines resolution and the x-ray throughput, i.e., the output count rate (OCR) vs. input count rate (ICR). Higher throughput comes at the expense of poorer resolution. Quantitative EDS analysis is typically performed under "best spectral resolution" conditions to maximize the spectral peak-to-background and to minimize peak interferences. For example, Si(Li)-EDS operation with best spectral resolution of 129 eV for a 10 mm^2 active area detector, where resolution is defined as the full peak width at half peak maximum intensity (FWHM) measured at MnKα (5890 eV), requires a time constant in the range 30 μs to 50 μs. This limits the maximum output count rate (OCR) to less than 2 kHz, giving a useful throughput of approximately 1 kHz at an acceptable detector deadtime (e.g., less than 40 percent). Thus, in a typical spectrum measurement of 100 seconds, the integrated spectral count would be approximately 100,000 for an Si(Li)-EDS quantitative analysis.

Recently, the EDS measurement situation has changed profoundly with the rapid introduction of the silicon drift detector energy dispersive x-ray spectrometer (SDD-EDS).[5,6] SDD-EDS outperforms Si(Li)-EDS in all critical aspects of analytical x-ray spectrometry except for the efficiency for high photon energies. [Above 10 keV photon energy, the greater thickness of the Si(Li)-EDS inevitably provides greater stopping power, e.g., at U Lα, (13.61 keV), a 3-mm thick Si(Li)-EDS is 100% efficient, while a 450 μm thick SDD-EDS is 70% efficient.] For the critical analytical parameters of optimum spectral resolution, resolution as a function of detector active area, peak stability (width and peak channel position), and low photon energy performance, SDD-EDS performance is modestly to significantly better than Si(Li)-EDS.[8] But for the most critical analytical parameter of detector throughput, e.g., resolution as a function of detector time constant, SDD-EDS greatly surpasses Si(Li)-EDS performance.[7] To achieve resolution below 130 eV (MnKα) typically requires a time constant of 500 ns or less for SDD-EDS compared to ~30 μs for Si(Li)-EDS. The maximum throughput of a single detector SDD-EDS can thus exceed the throughput of Si(Li)-EDS by a factor of at least 60 for similar EDS resolution (e.g., comparing commercially available EDS detectors, a particular 10 mm^2 SDD-EDS produces a maximum OCR of 130 kHz at a resolution of 127.5 eV (MnKα) compared to 1.9 kHz at 129 eV for Si(Li)-EDS).[7] Moreover, by assembling clusters of SDD detectors and combining the output, the total throughput can be increased to yield a maximum OCR above 500 kHz for a 4-detector SDD-EDS while maintaining a resolution of 127.5 eV. By choosing a shorter time constant (220 ns) that degrades the resolution to 145 eV, the single SDD-EDS detector can reach a maximum OCR of 270 kHz and the cluster can exceed 1.25 MHz. Thus, for the most critical parameter of detector throughput, the OCR vs. ICR performance of SDD-EDS greatly exceeds that of Si(Li)-EDS, and this level of performance directly translates into significant improvements in quantitative analysis by enabling collection of statistically robust EDS spectra in a practical measurement interval of 100 seconds or less.

The precision <u>and</u> accuracy of EDS analysis are both improved by processing high count spectra. Characteristic peak intensities are determined by multiple linear least squares (MLLS) peak fitting to extract the peak from the spectral background (arising from electron bremsstrahlung) and from interfering peaks arising from other elements. As a fitting model, MLLS utilizes a "peak reference", in effect the ideal peak(s) structure, obtained for each element/x-ray family from a measured spectrum known to be free of spectral interferences for the element of interest. By forming the peak reference from a high count spectrum, the channel-to-channel variation due to random counting statistics is minimized, creating a more robust reference. By applying a suite of robust peak references to high count spectra of unknowns and standards, the most accurate possible determination of characteristic peak intensities is obtained within the limitations of MLLS peak fitting. The measured intensities on unknowns and standards then are used to form k-values for subsequent matrix correction to yield concentrations. As an example of the level of quantitative analysis that can be achieved with high-count (5,000,000) spectra measured by SDD-EDS, Table 1 presents results from the analysis of 20 locations randomly selected on a polished bulk specimen of NIST Standard Reference Material (SRM) 470 (K411 glass).[8] Pure element standards were used for Mg, Si, and Fe, and SRM 470 (K412 glass) was selected for the Ca standard. The results agree with the SRM values within 1.7% relative, and the precision of a single measurement is 0.11% or less.

* The following definitions for classes of concentration, C, will be used in this paper:

"major" constituent: $C > 0.1$ mass fraction (10 weight percent)
"minor": $0.01 \leq C \leq 0.1$
"trace": $C < 0.01$

Table 1 SDD-EDS Analysis of SRM 470 (K411 glass) as ideal polished bulk target (20 analyzed locations); values in weight percent; (E_0 = 20 keV; 50 s spectra; ~5,000,000 x-ray counts from 0.1 keV to 20 keV))

	O (stoichiometry)	Mg	Si	Ca	Fe
Average (20)	42.87	8.76	25.77	11.20	11.40
Std. Dev.	0.022	0.045	0.053	0.026	0.031
SRM value (%)	42.36	8.85	25.38	11.06	11.21
Relative Error (%)	+1.2	-1.0	+1.5	+1.3	+1.7
Relative standard deviation (%) (20)		0.5	0.21	0.23	0.275
Single measure, Relative σ_C (%)		0.11	0.079	0.089	0.26

One of the critical requirements to satisfy the standards-based k-value measurement protocol concerns the geometry of the specimen and standard(s), all of which must be in the form of a flat, polished bulk target placed at carefully defined angles to the incident beam and the x-ray spectrometer. Such a well-defined specimen geometry is often not available to the SEM analyst whose specimens are frequently rough and irregular or are in the form of particles and other features where the dimensions approach those of the electron interaction volume and the x-ray generation /propagation ranges. Nevertheless, EDS spectra can usually be readily obtained from such irregular specimens examined in the SEM, and the k-value analytical protocol, or other analytical protocols such as the 'standardless' method, can be performed to give concentrations, which are typically examined as normalized concentrations. But how useful are such measurements in terms of the reliability of the results? This paper considers the impact of a range of specimen geometries that depart from the ideal flat, polished bulk material case but which represent some of the types of realistic specimens encountered in practical applications of SEM/EDS.

2. METHODOLOGY**

For the study of specimen shape effects, a JEOL 8500F thermal field emission gun electron probe microanalyzer was used as the SEM imaging platform, and a Bruker QUAD SDD-EDS, consisting of four 10 mm^2 detectors with summed output, was used for x-ray spectrometry. The Bruker QUAD SDD-EDS was operated with the intermediate speed time constant (440 ns), which provided a peak OCR of approximately 130 kHz per detector, or 520 kHz for the cluster, at a measured resolution of 127.5 eV (MnKα). To provide efficient excitation of the analytical photon energy range from approximately 100 eV to 12 keV, an incident beam energy of 20 keV was chosen and the beam current was selected to provide an OCR of approximately 100 kHz at a system deadtime of approximately 10% or lower to minimize the contribution of coincidence peaks to the spectrum. Spectra of unknowns and standards were collected for 50 s giving a spectrum integral (0.10 keV – 20 keV) of approximately 5 million counts. The spectra were evaluated with the NIST DTSA-II advanced x-ray spectrum processing software platform.[9] The multiple linear least squares (MLLS) peak fitting procedure in DTSA-II was used to extract the characteristic peak intensities. MLLS peak references were measured on pure elements for Mg, Si, and Fe and on $CaCO_3$ for Ca to ensure that there were no peak interferences corrupting the peak references. Intensity measurements on samples and standards were used to form k-values, and concentrations were calculated from the suite of k-values with the XPP matrix correction procedure embedded in DTSA-II. Standards utilized included elemental Mg, Si, and Fe, and NIST SRM 470 (K412 glass) for Ca.[9] The oxygen constituent was not directly measured but was calculated by the method of assumed stoichiometry of the cations, with Fe assigned a valence of 2.

** Disclaimer: Certain commercial equipment, instruments, or materials are identified in this paper to foster understanding. Such identification does not imply recommendation or endorsement by the National Institute of Standards and Technology, nor does it imply that the materials or equipment identified are necessarily the best available for the purpose.

NIST SRM 470 (K411 glass), the composition of which is listed in Table 2, was chosen for this study of specimen geometry effects because the elemental composition provided characteristic x-ray peaks that spanned a wide range of photon energy and the brittle nature of the glass enabled creation of different geometric forms by simple mechanical means. The geometric effects of size, shape, surface roughness, and local surface inclination have different impacts depending on the x-ray photon energy, with low energy x-rays below a photon energy of approximately 4 keV being particularly susceptible to changes in the x-ray absorption path to reach the detector, while the generation of higher energy photons is more strongly affected by the loss of high energy electrons due to anomalous beam penetration or scattering effects. The bulk glasses (K411 and K412 to serve as a Ca standard) were prepared metallographically to create highly polished surfaces. Surface cavities occasionally produced by fracturing during grinding and subsequently preserved through the polishing sequence were selected as an example of a severe specimen geometry. To create a variety of different specimen geometries, K411 glass was modified by abrading the previously polished surface of a K411 block with 600-grit silicon carbide grinding paper to produce directional striations. Bulk K411 was mechanically crushed to produce coarse shards (dimensions of several millimeters) and with further grinding to produce microscopic irregularly-shaped particles (dimensions of tens of micrometers), which were mounted on conducting adhesive tape. All polished specimens as well as the special geometric forms materials were coated with 7 nm of carbon by thermal evaporation with specimen rotation during the coating procedure to minimize shadowing.

Table 2 SRM 470 (K411 glass)

Element	SRM Concentration (weight percent)	K-L3 (“Kα”) Energy (keV)
O	42.36	0.523
Mg	8.85	1.254
Si	25.38	1.740
Ca	11.06	3.690
Fe	11.21	6.400

3. RESULTS

3.1 Ideal polished bulk K411 glass

Using the data set summarized in Table 1, Figure 1 shows a plot of the Mg concentration (normalized) versus the Fe concentration (normalized) for 20 randomly selected fixed-beam analyses performed on polished bulk K-411 glass, the ideal specimen shape to satisfy the rigorous k-value measurement protocol. The estimated precision (one-sigma) of the concentration based on the x-ray count for each element and standard is also shown. With one exception, the results cluster within approximately 1 percent relative of the mean for both elements. The exception outside this cluster is approximately 2 percent below the mean for both constituents, and examination of the complete analysis at this location reveals a compensating excess in Si, which suggests a real deviation in composition at this location in an otherwise homogeneous material. The deviation of the mean values from the certified composition of K411 is -1.0% relative for Mg (8.76% measured vs SRM 8.85%) and +1.8% relative for Fe (11.40% measured vs. SRM 11.21%). In the subsequent examples for different specimen shapes, the results from the ideal flat bulk material are plotted as a reference.

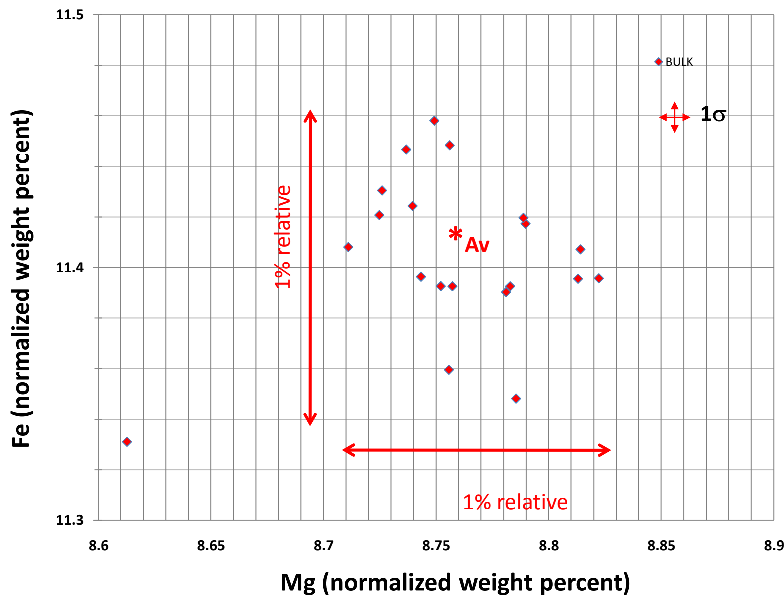

Figure 1 Analysis of polished bulk K411 glass: plot of Fe concentration (normalized) vs. Mg concentration (normalized). The average and the 1σ range based on counting statistics are shown.

3.2 Bulk K411 glass abraded with 600 grit SiC

Figure 2 shows an SEM secondary electron image (Everhart-Thornley detector, positively biased) of a typical area after abrading with 600 grit SiC to produce a series of roughly parallel scratches oriented perpendicular to the SDD-EDS axis. The brittle nature of the glass results in local fracturing during the abrading process, creating an irregular surface with relief extending to tens of micrometers. Figure 3 shows a plot of 20 fixed-beam analyses performed on abraded K-411 glass within features such as that shown in Figure 2. The range of relative errors is greatly expanded over the ideal bulk case shown in Figure 2.

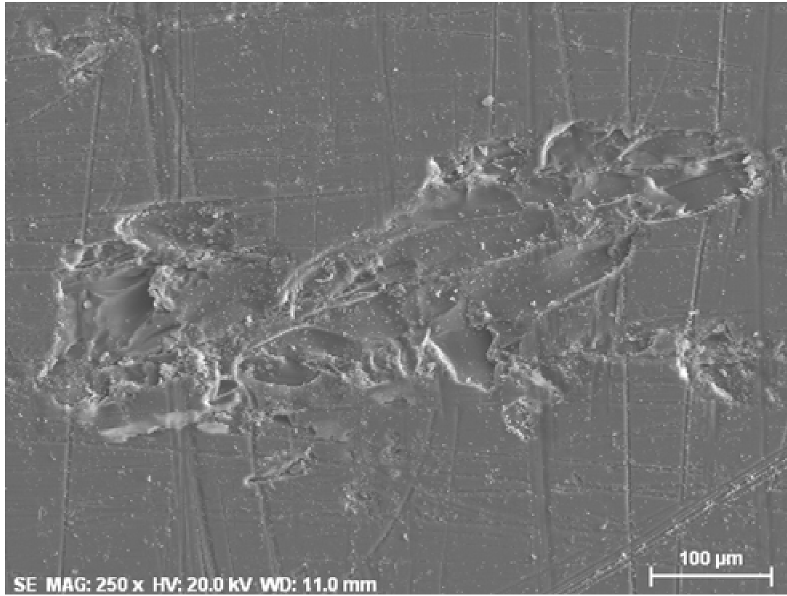

.

Figure 2 SEM secondary electron image of K411 glass after abrasion with 600 grit SiC.

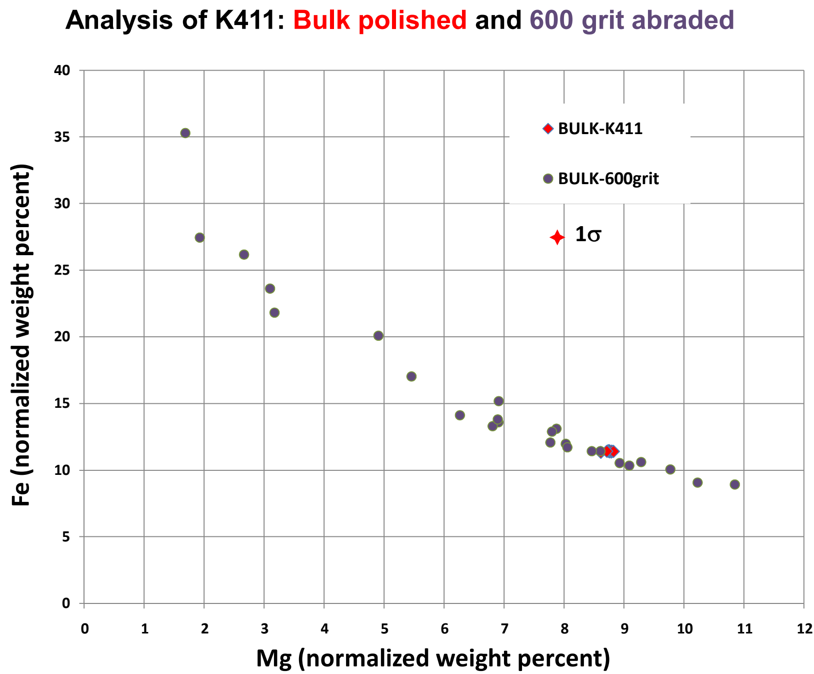

Figure 3 Analysis of bulk K411 glass after abrasion with 600 grit SiC: plot of Fe concentration (normalized) vs. Mg concentration (normalized). The 1σ range based on counting statistics is also shown as the red cross.

3.3 Surface voids in bulk K411 glass

Figure 4 shows examples of surface voids that remain after final polishing of bulk K411 glass. Fixed-beam analyses were performed at various locations within these voids, and the results are shown in Figure 5.

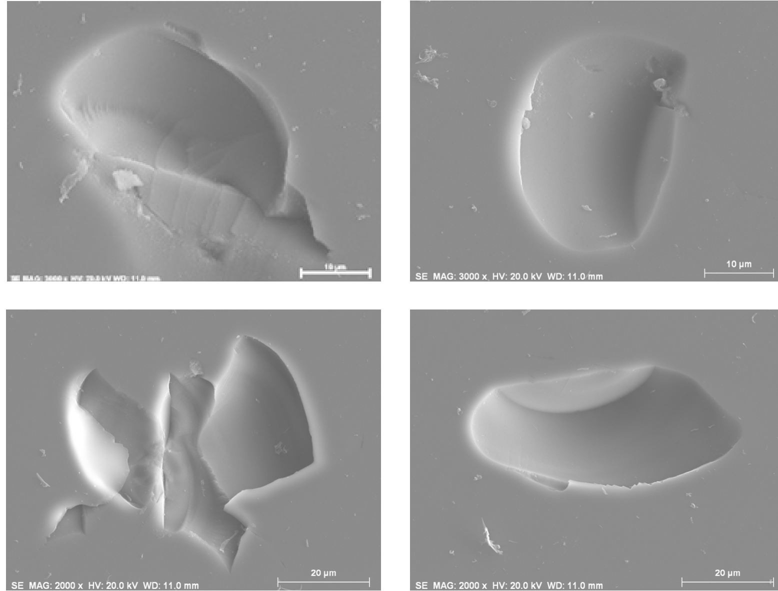

Figure 4 SEM secondary electron images of surface voids in K411 glass remaining after final polishing.

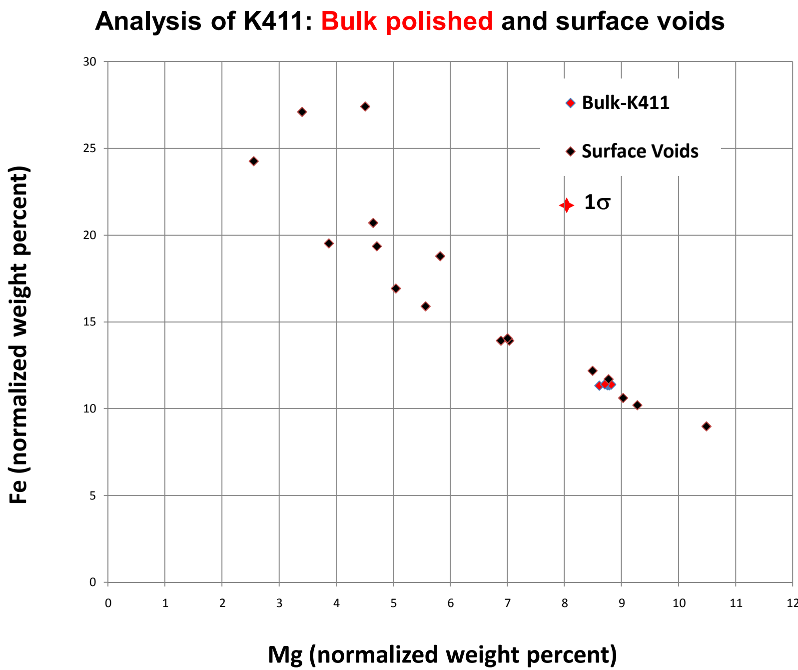

Figure 5 Analysis of surface voids in bulk K411 glass remaining after final polishing.

3.4 Macroscopic shards

Figure 6 shows examples of macroscopic chips formed by fracturing bulk K411 glass. Fixed-beam analyses were performed at various locations on these chips, and the results are shown in Figure 7.

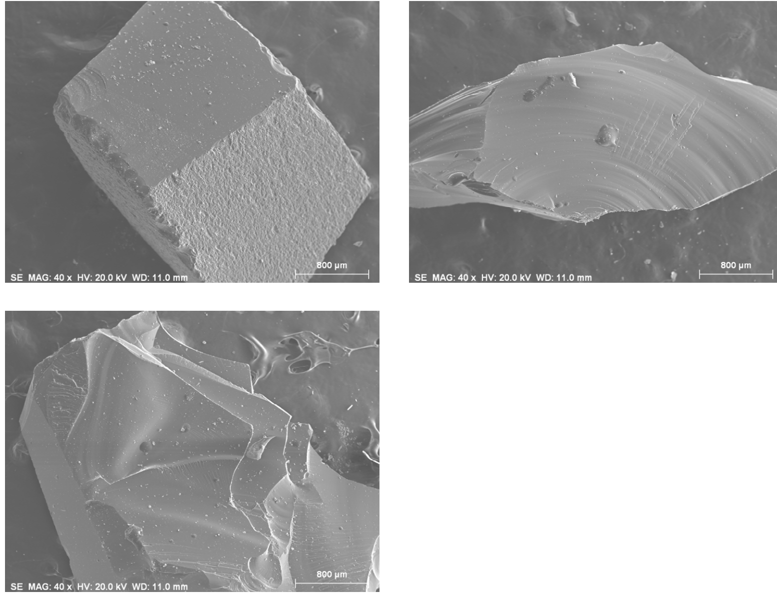

Figure 6 SEM secondary electron images of macroscopic chips of bulk K411 glass after fracturing.

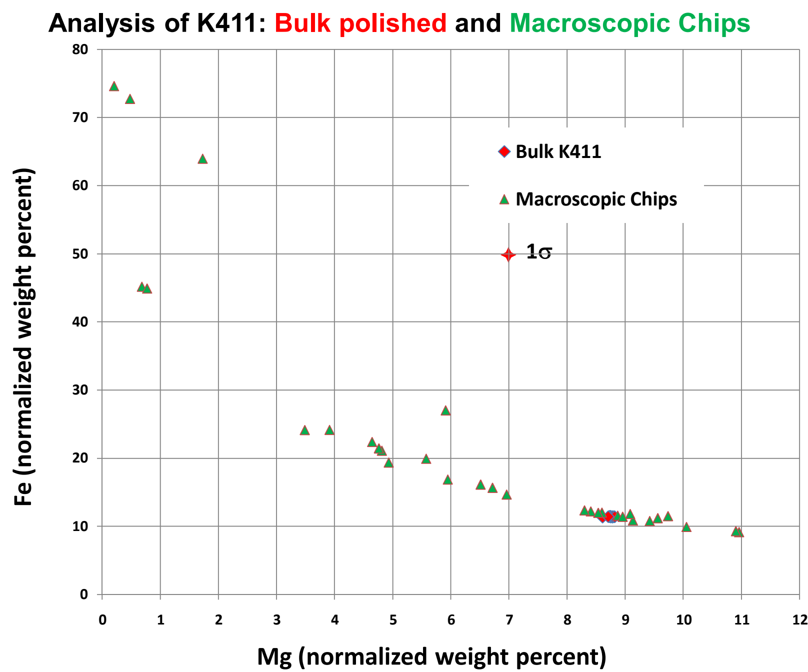

Figure 7 Fixed-beam analysis of macroscopic chips of K411 glass.

3.5 Microscopic fragments of K411 glass

Figure 8 shows examples of microscopic shards of K411 glass prepared by dry milling. Analyses were performed on these shards using two different beam strategies: fixed-beam analysis at the approximate center of the particle with the results in Figure 9, and continuous scanning with a scan field selected to bracket the particle, shown in Figure

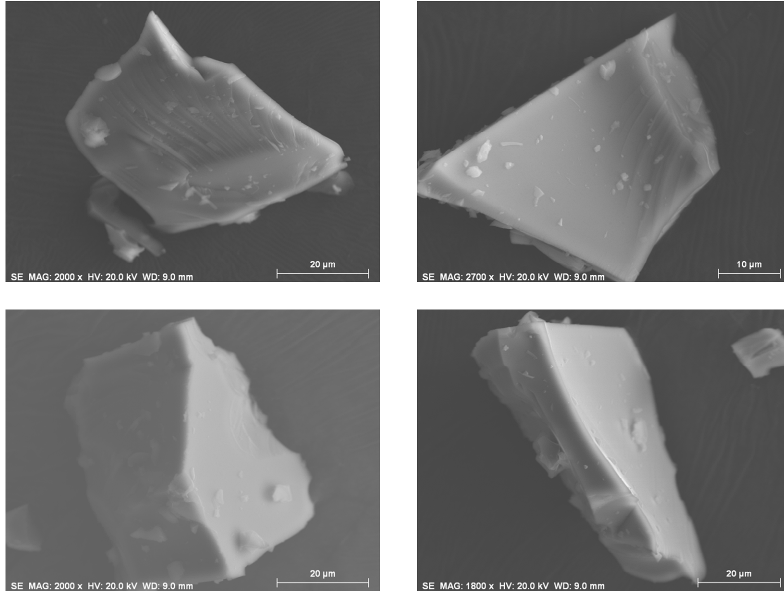

10.

Figure 8 SEM secondary electron images of macroscopic chips of bulk K411 glass after fracturing.

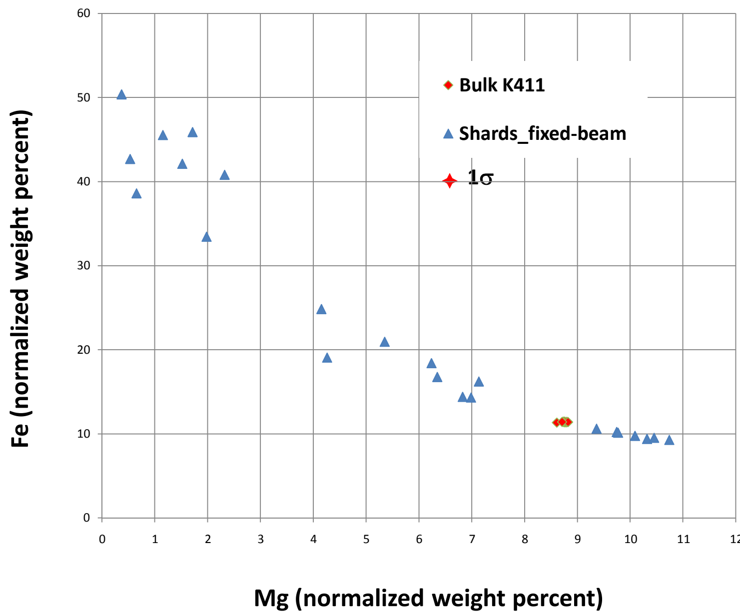

Figure 9 Fixed-beam analysis of microscopic shards of K411 glass.

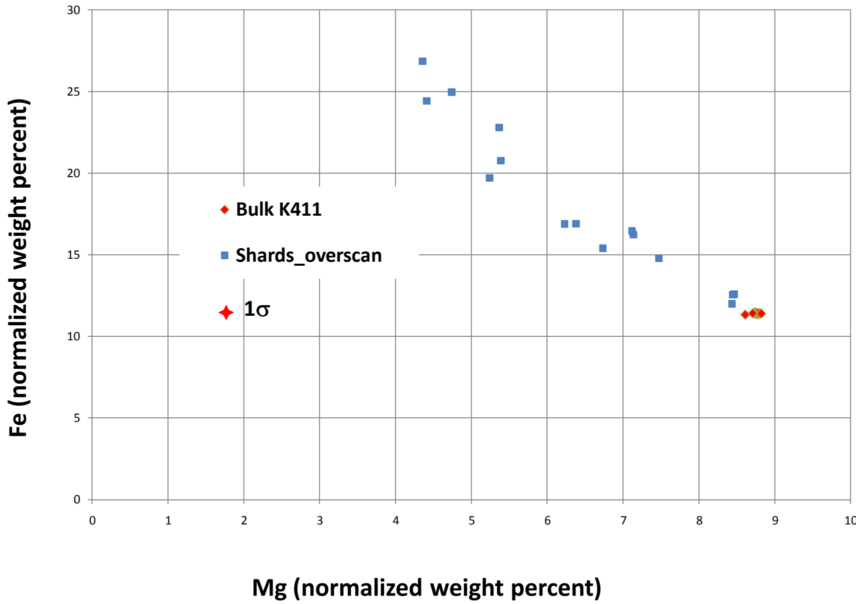

Figure 10 Bracketing-scan analysis of macroscopic shards of K411 glass.

4. DISCUSSION

Mg and Fe have been chosen for this study because their wide separation in photon energy, e.g., MgKα,β (photon energy 1.254 keV) and FeKα (6.400 keV), results in sharply different responses to geometric effects:

The generated x-ray intensity, I_g, depends strongly on the overvoltage U, where $U = E_0/E_c$, E_0 is the incident beam energy and E_c is the critical excitation energy ("absorption energy", "ionization energy"):

$$I_g \sim (U - 1)^{1.67}$$

This exponential dependence causes higher energy photons, which for a given choice of E_0 are excited at lower overvoltage, to be more sensitive to the loss of high energy beam electrons through enhanced backscattering from highly tilted surfaces or from enhanced beam penetration through specimens with microscopic dimensions.

X-ray absorption depends strongly on the materials present and the path length through the specimen:

$$I/I_0 = \exp [-(\mu/\rho)\, \rho s)]$$

where I_0 is the original intensity, I is the intensity after propagation along a path length s, ρ is the density, and μ/ρ is the mass absorption coefficient. In a given material, low energy photons less than approximately 4 keV are more strongly absorbed compared to higher energy photons and are therefore especially sensitive to changes in the absorption path length out of the specimen that result from modifications to the specimen geometry from the ideal flat bulk case. Situations can occur where the path length is greater than that for the polished bulk target, such as a beam location at the bottom of a hole, leading to enhanced absorption and selective loss of low energy photons. Alternatively, the path length to escape may be reduced compared to the flat bulk target, such

as the case of a microscopic particle where the local surface curvature shortens the escape path, leading to reduced absorption and a relative enhancement in intensity for low energy photons.

Each of the geometric shapes tested in this paper produced a strong deviation of the analyzed composition from the true value. Figure 11summarizes the results for all of the materials. A microscopically homogeneous material which can be analyzed by SDD-EDS within 2 percent relative of the SRM values when it is in the ideal flat bulk shape shows a huge range of error when geometric effects occur, a factor of 10 or more for some shapes. The impact of geometric factors on the range of the measured concentrations is so great as to render the quantitative results of little value for most practical uses, such as identifying a material or making comparisons of a process that produces products with different physical shapes.

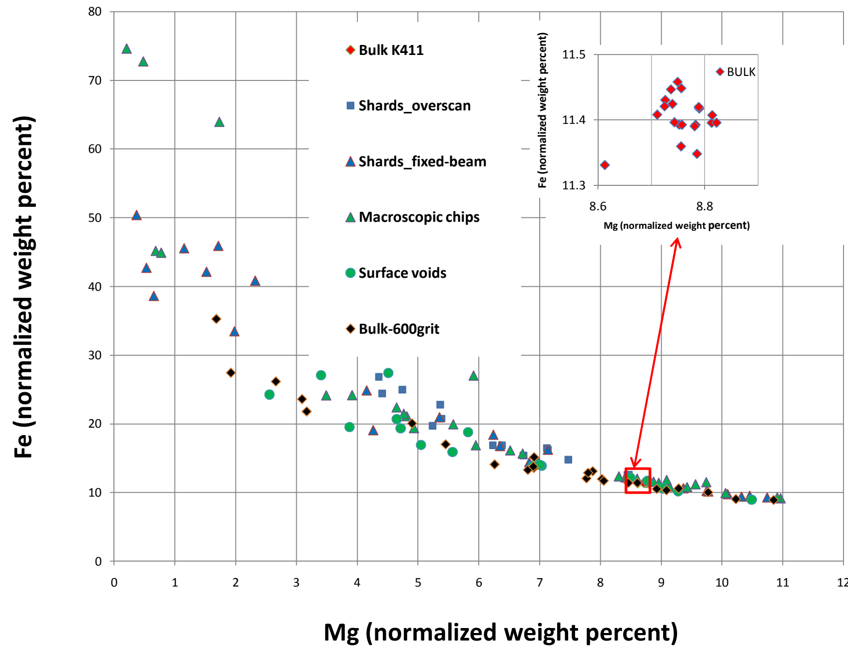

Figure 11 Summary of all results for K411 glass.

What can the analyst who is confronted with the problem of analyzing rough, irregularly shaped specimens that cannot be prepared as ideal polished flat bulk targets do to minimize the impact of the geometric factors on the error range? There are at least three procedures/protocols to consider:

1. The analytical total

When quantitative x-ray microanalysis is performed following the rigorous standards-based k-value protocol, each element is determined against a pure element standard or its equivalent under conditions of identical, or known and scalable, dose. While this k-value measurement is strictly a relative rather than an absolute determination, by controlling the dose and spectrometer efficiency and using a suite of standards that effectively establishes a reference quantity of measured mass for each element. The concentrations so determined can be meaningfully compared to absolute analytical values, e.g., the reference analytical procedures used to determine the overall composition of the Standard Reference Materials used in this study. Moreover, if all elements are measured (with the possible exception of oxygen which can be calculated based on the assumed stoichiometry of the cation species) and the undetectable elements H, He, and Li are not present, then the raw, un-normalized analytical total of all the constituents contains useful and important information.[1] Considering the impact of the systematic errors that are inherent in the k-value/matrix correction quantification scheme, the analytical total can be reasonably expected to lie within a range of 98% to 102% for most analyses. Deviations outside this range are indicative of the impact of factors other than composition on the

measurement process, such as the geometric effects encountered in this study. Figures 12 and 13 show plots of the Fe and Mg concentrations (normalized) versus the raw analytical total. The deviation of the normalized concentration from the correct value is strongly correlated with the analytical total, with the relative errors for each element falling within about 20% or less of the correct value provided that the raw analytical total is in the range 80% to 120%. Thus, by following the k-value protocol and monitoring the analytical total, the analyst obtains a strong indication of the broadened error range to which a particular analysis may be vulnerable.

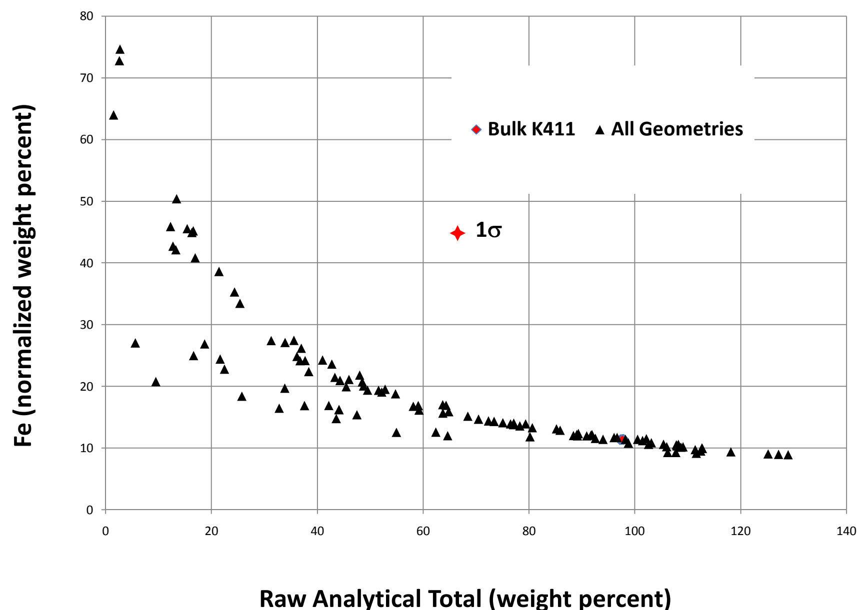

Figure 12 Fe concentration (normalized weight percent) vs. analytical total

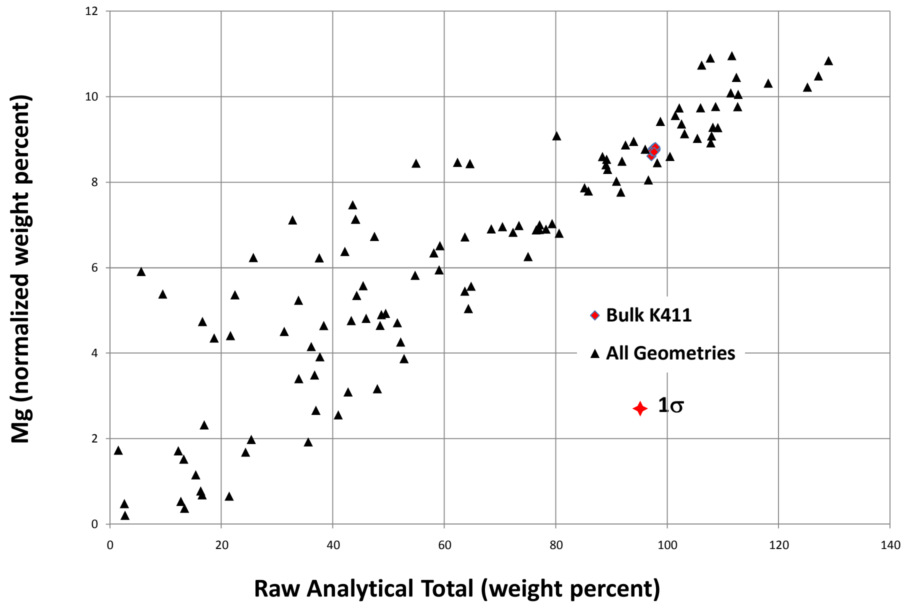

Figure 13 Mg concentration (normalized weight percent) vs. analytical total

In recognizing the utility of the analytical total, it must be noted that the use of the "remote-standards standardless" analysis procedure available in most commercial x-ray microanalysis software systems precludes the use of the analytical total as an indicator of the possible severity of geometric effects or any other deviations from the ideal measurement protocol. [10] The "remote-standards standardless" analysis procedure derives a suite of standard intensities as needed from a library of standard measurements made on another instrument. Calculated corrections based upon the measurement physics are made for differences in beam energy and spectrometer efficiency between the local instrument and the remote library instrument, but there is no dose calibration attempted so the raw analytical total has no validity. Normalization must be applied to place the calculated concentrations on a sensible basis, thus losing any indication of the influence of other factors possibly affecting the analytical total.

2. Examination of the EDS spectrum shape

The impact of anomalous absorption, particularly in the low energy region of the x-ray spectrum, can be observed directly in the EDS spectrum when a channel-by-channel comparison is made to the spectrum of the same material in the form of a flat bulk target. The x-ray continuum which forms the background provides intensity at every photon energy up to the Duane-Hunt limit set by the incident beam energy. Figure 14 shows a comparison of the spectrum of ideal flat bulk K411 and several spectra from microscopic particle shards. The background near each low photon energy peak provides a direct indication of how severely that peak differs from the ideal case. The large deviation from the ideal spectrum is readily apparent for these shards and should serve as a warning that applying conventional k-value/matrix corrections to such a spectrum followed by normalization is likely to lead to unacceptably large errors. The obvious problem in using this tool for the analysis of unknowns is the lack of a reference spectrum from a flat, bulk target of the appropriate composition, since this composition is the objective of the analysis. A possible solution is to simulate the bulk reference spectrum from an estimate of the composition of the unknown using a software tool such as NIST DTSA-II which calculates the spectrum on a first principles basis to yield absolute intensities.[9] Figure 15 shows an example of measured and simulated spectra for bulk K411 at E_0 = 20 keV. No scaling has been applied to the simulation, and the estimate of the sum of the characteristic peak and background intensities ranges from +1.2% relative at FeKα to +19% relative at MgK. When simulating an unknown composition, a useful first estimate of composition can be obtained from the first normalized analysis.

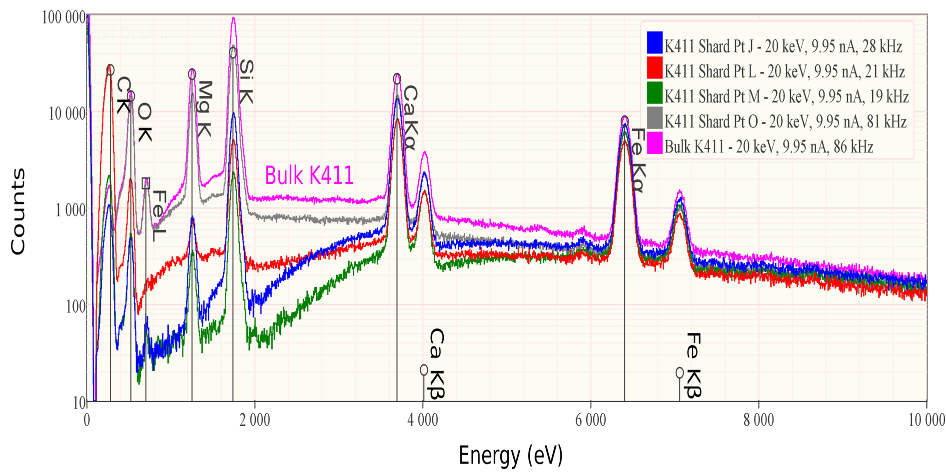

Figure 14 SDD-EDS spectra of bulk K411 and various microscopic shards (fixed-beam analysis)

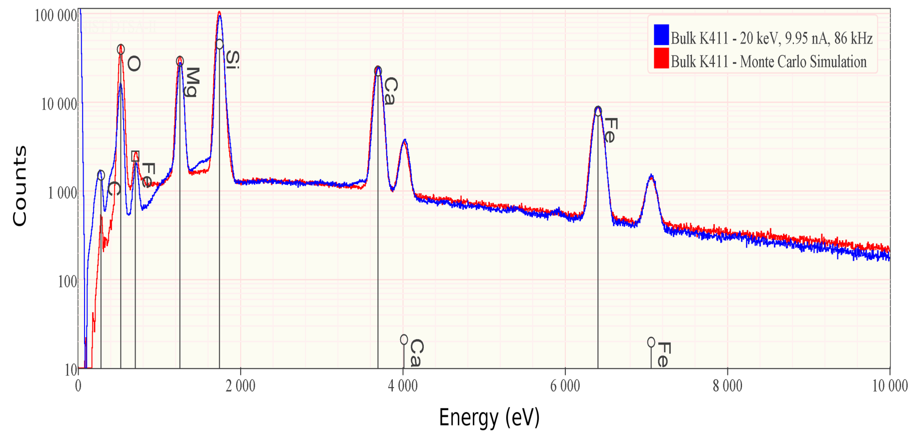

Figure 15 Comparison of bulk K411 as measured (blue) and as simulated (red) with NIST DTSA-II.

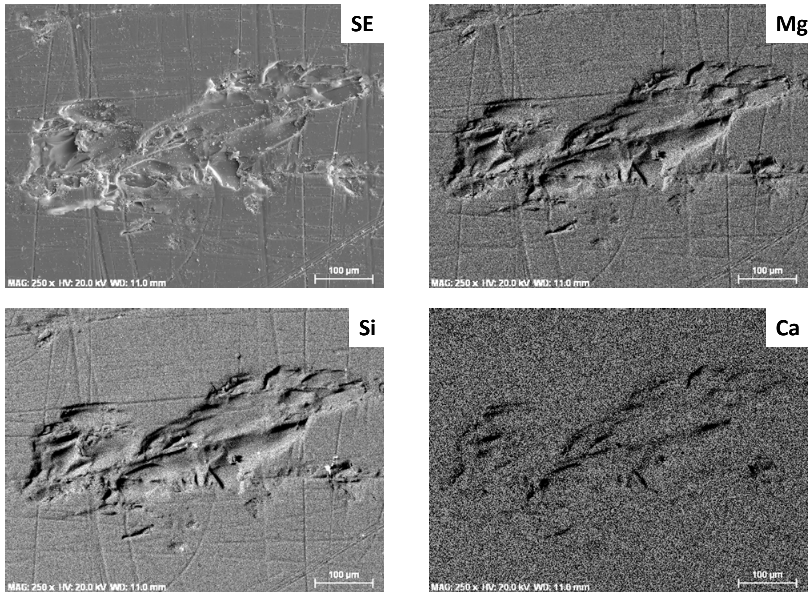

Figure 16 Secondary electron and x-ray intensity images recovered from an x-ray spectrum image of a damaged area after abrasion with 600 grit SiC.

3. X-ray spectrum imaging

The high throughput of SDD-EDS makes it advantageous to collect x-ray microanalysis data of geometrically complex targets in the x-ray spectrum imaging (XSI) mode, in which at each pixel of an x-y scan a complete SDD-EDS spectrum is recorded.[8] The x-y-I(E) database thus created can be interrogated by software tools in various ways, including forming x-ray intensity images that can directly reveal areas of anomalous absorption, as shown in the example of Figure 16. The analyst can then use software tools to recover summed spectra from groups of contiguous pixels located in these favorable locations for subsequent quantitative analysis.

5. CONCLUSIONS

The throughput of SDD-EDS enables the analyst to obtain high count spectra, 5 to 10 million integrated counts, with modest time expenditures, 100 s or less per analysis location. When combined with the k-value standardization and matrix correction protocol, these high count spectra form the basis for robust high precision and high accuracy analysis equivalent to that achieved with WDS. While EDS can be as accurately quantitative as WDS for specimens in the form of flat polished bulk targets, this level of analytical performance can be greatly compromised for non-ideal specimen shapes. Specimens examined in the SEM frequently have strong geometric shape effects on EDS measurements that lead to a much broader error range compared to that encountered with ideal polished bulk specimens. The careful analyst following the k-value/matrix correction protocol can make use of raw analytical total, the low photon energy spectrum shape, and direct mapping in the x-ray spectrum imaging mode to recognize the most favorable locations on rough, irregular specimens to choose for analysis so that the quantitative results are subject to the minimum errors.

REFERENCES

[1] Goldstein, J., Newbury, D., Joy, D., Lyman, C., Echlin, P., Lifshin, E., Sawyer, L., and Michael, J., Scanning Electron Microscopy and X-ray Microanalysis, 3rd edition, Springer, New York, 1-19 (2003).

[2] Heinrich, K.F.J., Electron Beam X-ray Microanalysis, Van Nostrand Reinhild, New York (1981) 99-140.

[3] Fitzgerald, R., Keil, K. and Heinrich, K., “Solid-state energy-dispersion spectrometer for electron-microprobe x-ray analysis”, Science 159, 528- (1968).

[4] Fiori, C., Myklebust, R., Heinrich, K., and Yakowitz, H., Analytical Chemistry, 48, 172 (1976).

[5] Struder, L., Fiorini, C., Gatti, E., Hartmann, R., Holl, P., Krause, N., Lechner, P., Longoni, A., Lutz, G., Kemmer, J., Meidinger, N., Popp, M., Soltau, H., and von Zanthier, C. Mikrochim. Acta [suppl.] 15, 11-19 (1998)

[6] Newbury, D., “Electron-Excited Energy Dispersive X-Ray Spectrometry at High Speed and at High Resolution: Silicon Drift Detectors and Microcalorimeters”, Microsc. Microanal. 12 (2006) 527–537.

[7] Newbury, D. “The Revolution in Energy Dispersive X-ray Spectrometry: Spectrum Imaging at Output Count Rates Above 1 MHz with the Silicon Drift Detector on a Scanning Electron Microscope”, Spectroscopy, 24, 32-43 (2009).

[8] National Institute of Standards and Technology Standard Reference Materials Program, information at http://www.nist.gov/srm/index.cfm

[9] Ritchie, N., “Getting Started with NIST DTSA-II”, Microsc. Today, (19) 2011 26-31; DTSA-II is available for free download at www.cstl.nist.gov/div837/837.02/epq/dtsa2/index.html

[10] Newbury, D. E., Swyt, C. R., and Myklebust, R. L., "'Standardless' Quantitative Electron Probe Microanalysis with Energy-Dispersive X-ray Spectrometry: Is It Worth the Risk?", Analytical Chemistry, 67 (1995) 1866-1871.

* Certain commercial equipment, instruments, or materials are identified in this paper to foster understanding. Such identification does not imply recommendation or endorsement by the National Institute of Standards and Technology, nor does it imply that the materials or equipment identified are necessarily the best available for the purpose.